LUND UNIVERSITY

Generation of human pluripotent stem cell reporter lines for the isolation of and reporting on astrocytes generated from ventral midbrain and ventral spinal cord neural progenitors.

Holmqvist, Staffan; Brouwer, Marinka; Djelloul, Mehdi; Diaz, Alejandro Garcia; Devine, Michael J; Hammarberg, Anna; Fog, Karina; Kunath, Tilo; Roybon, Laurent

Published in:
Stem Cell Research

DOI:
10.1016/j.scr.2015.05.014

2015

Stem Cell Research (2015) 15, 203–220

Available online at www.sciencedirect.com

ScienceDirect

www.elsevier.com/locate/scr

METHODS AND REAGENTS

Generation of human pluripotent stem cell reporter lines for the isolation of and reporting on astrocytes generated from ventral midbrain and ventral spinal cord neural progenitors

Staffan Holmqvist[a,b], Marinka Brouwer[a,b], Mehdi Djelloul[a,b], Alejandro Garcia Diaz[c], Michael J. Devine[d,e], Anna Hammarberg[f], Karina Fog[g], Tilo Kunath[d], Laurent Roybon[a,b,*]

[a] *Stem Cell Laboratory for CNS Disease Modeling, Wallenberg Neuroscience Center, Department of Experimental Medical Science, Lund University, BMC A10, 22184, Lund, Sweden*
[b] *Strategic Research Area MultiPark and Lund Stem Cell Center, Lund University, 22184, Lund, Sweden*
[c] *Columbia Stem Cell Core Facility, 650 West 168th Street, New York, NY 10025, USA*
[d] *MRC Centre for Regenerative Medicine, Institute for Stem Cell Research, University of Edinburgh, Edinburgh EH16 4UU, UK*
[e] *Department of Molecular Neuroscience, UCL Institute of Neurology, Queen Square, London WC1N 3BG, UK*
[f] *MultiPark Strategic Research Area, Cellomics and Flow Cytometry Core Facility, Department of Experimental Medical Science, Lund University, BMC B12, 22184, Lund, Sweden*
[g] *H. Lundbeck A/S, Valby, Denmark*

Received 9 January 2015; received in revised form 28 May 2015; accepted 28 May 2015
Available online 6 June 2015

Abstract
Astrocytes play a critical role during the development and the maintenance of the CNS in health and disease. Yet, their lack of accessibility from fetuses and from the brain of diseased patients has hindered our understanding of their full implication in developmental and pathogenic processes. Human pluripotent stem cells (PSCs) are an alternative source to obtain large quantities of astrocytes *in vitro*, for mechanistic studies of development and disease. However, these studies often require highly pure populations of astrocytes, which are not always achieved, depending on the PSC lines and protocols used. Here, we describe the generation and characterization of human PSC reporter lines expressing TagRFP driven by the *ABC1D* region of the human *GFAP* promoter, as new cellular model for generating homogenous population of astrocytes generated from CNS regionally defined PSC-derived neural progenitors. *GFA_{ABC1D}::TagRFP*-expressing astrocytes can be purified by fluorescent-activated cell sorting and maintain a bright expression for several additional weeks. These express canonical astrocyte markers NF1A, S100β, CX43, GLAST, GS and CD44. These new cellular models, from which highly pure populations of

* Corresponding author at: Stem Cell Laboratory for CNS Disease Modeling, Department of Experimental Science, MultiPark and Lund Stem Cell Center, Lund University, BMC A10, Sölvegatan 19, SE-221 84 Lund, Sweden.
E-mail address: Laurent.Roybon@med.lu.se (L. Roybon).

http://dx.doi.org/10.1016/j.scr.2015.05.014

fluorescence-expressing astrocytes can be obtained, provide a new platform for studies where pure or fluorescently labeled astrocyte populations are necessary, for example to assess pro-inflammatory cytokine and chemokine release in response to specific treatment, and uptake and degradation of fluorescently labeled pathogenic proteins, as reported in this study.

Introduction

Astrocytes are the most abundant cell type in the human brain. They play a critical role in the maintenance of homeostasis of the central nervous system (CNS) by a wide spectrum of functions. These functions include, but are not restricted to, regulation of blood flow (Attwell et al., 2010), regulation of energy reserves (Choi et al., 2012), modulation of synaptic transmission (Simard and Nedergaard, 2004), neuronal connectivity (Eroglu and Barres, 2010), and uptake of potentially pathogenic proteins (Lee et al., 2010; Wakabayashi et al., 2000). Furthermore, astrocytes can be triggered by environmental cues including cytokines and chemokines to become reactive during brain injury (Chen and Swanson, 2003) and neurodegenerative diseases, such as amyotrophic lateral sclerosis (Haidet-Phillips et al., 2011; Yamanaka et al., 2008) and Parkinson's disease (Waak et al., 2009). Although these reactive astrocytes are thought to have a neuroprotective function, astrocyte reactivity has also been associated with neurotoxicity (Chao et al., 1996; Episcopo et al., 2013; Lee et al., 2013; Pekny et al., 2014); the mechanisms of balance between neuroprotection and neurotoxicity are still not well understood.

During human brain development, neuroepithelial cells are subject to regional patterning through the effects of morphogens such as retinoic acid (RA) or sonic hedgehog (SHH) (Kiecker and Lumsden, 2012; Rowitch and Kriegstein, 2010). Neuroepithelial cells have the potential to differentiate into glial cell types (astrocytes and oligodendrocytes) and distinct neuronal subtypes characterized by the neurotransmitter they release and expression of regional identity markers. Recent work has evidenced that positional diversity also exists among astrocytes (Tsai et al., 2012), therefore raising a growing interest in the effects of patterning factors during the development of astrocytes. Moreover, there is increasing evidence that astrocytes may differ between brain structures, and within these structures, depending on their location along the dorso-ventral and rostro-caudal axis (Anderson et al., 2014; Bachoo et al., 2004; Chaboub and Deneen, 2012). Because primary human material is not always accessible, advance in the understanding of astrocyte development and diversity has mainly been based on observations in rodent models (Deneen et al., 2006; Hochstim et al., 2008), and it is only recently that investigations using human astrocytes have been made to better characterize their functional properties, *in vivo* (Han et al., 2013; Oberheim et al., 2009).

One of the few feasible sources to investigate human astrocyte development and function in health and disease is via human pluripotent stem cells (PSCs). Human PSCs include embryonic stem cells (ESCs) and induced pluripotent stem cells (iPSCs) which often are the primary source of material used to study neuronal subtypes *in vitro* using protocols that include time-specific exposure to patterning cues following developmental principles (Hu et al., 2010; Swistowski et al., 2010). Recently, different protocols have also been described for the differentiation of human PSCs into regionalized astrocytes *in vitro* (Jiang et al., 2013; Juopperi et al., 2012; Kondo et al., 2013; Krencik et al., 2011; Roybon et al., 2013; Serio et al., 2013; Shaltouki et al., 2013; Yuan et al., 2011). However, as opposed to the multitude developed for generating spinal cord astrocytes (Jiang et al., 2013; Krencik et al., 2011; Roybon et al., 2013; Serio et al., 2013), only few exist for generating forebrain and midbrain astrocytes (Juopperi et al., 2012; Kondo et al., 2013; Krencik et al., 2011). The efficiency of these protocols to generate astrocytes, however, varies greatly not only depending on the type of PSCs primarily used, but also in-between individual iPSC lines generated from one or multiple patients. With PSC technologies potential to personalize medical therapy in the near future, there is a need for tools that can provide a reliable source of homogenous astrocyte populations, regardless of the primary material, enabling development of cellular models for the study of astrocytes maintenance of brain homeostasis in health and disease.

Acquiring an enriched population of a given cell type using a fluorescence-based reporter line has many advantages but requires that the reporter expression is specific to the cell type to be enriched. Glial fibrillary acidic protein (GFAP) is a well-known marker for astrocytes; its expression is dynamic, and associated with astrocyte differentiation (Brenner, 1994; Lee et al., 2008) and known to be up-regulated in reactive astrocytes, *in vitro*. Therefore, the GFAP promoter is a good candidate for the generation of astrocyte specific reporter lines for use in developmental and disease related *in vitro* studies. The human GFAP promoter consists of four distinct domains: A, B, C and D (Lee et al., 2008). Exclusion of the entire C-domain results in misexpression of GFAP and loss of astrocyte specific expression while maintenance of one of the six C-subdomains, the C_1-subdomain, allows astrocyte specific expression of GFAP throughout the CNS. Notably, this GFA_{ABC1D} element of the GFAP promoter is advantageous not only because of its reduced size but also since reporter driven expression by the GFA_{ABC1D} promoter was shown to be more efficiently expressed compared to when driven by the full size promoter (Lee et al., 2008). This streamlined promoter was previously successfully used to direct enhanced green fluorescent protein and short hairpin RNA in astrocytes (Yan et al., 2012).

In this study, we engineered human PSCs to express the monomeric red fluorescent protein (TagRFP) under the control of the human GFA_{ABC1D} promoter fragment (*GFA_{ABC1D}::TagRFP*). We initiated our work in human ESCs, and validated the reporter expression in astrocytes generated from human ESC-derived midbrain and spinal cord progenitors. Furthermore, we show that labeled astrocytes aged 90 DIV can be purified by FACS, and kept for an additional 40 days *in vitro* with no dramatic loss of reporter

expression. Additionally, we confirm the identity of our purified labeled astrocytes by immunocytochemistry for known astroglial markers nuclear factor 1 A-type (NF1A), S100 calcium-binding protein B (S100β), gap junction alpha-1 protein also known as Connexin 43 (CX43), Glutamate aspartate transporter (GLAST), Glutamine synthetase (GS) and cluster of differentiation protein 44 (CD44). As examples on how these labeled astrocytes can be used, we assessed secretion of pro-inflammatory mediators in enriched astrocyte cultures treated with fetal bovine serum (FBS) or IL-1β, and uptake and degradation of pathogenic proteins in non-purified astrocyte cultures, the latter substantiating the usefulness of our models for the tracking of pathogenic labeled proteins specifically in astrocytes. Finally, we demonstrate that our protocol for generating fluorescence-based ESC reporter lines is applicable to iPSCs. Both robustness and easiness of our method for generating hPSC reporter lines by transgenesis should facilitate the generation of many more cellular models for studies where homogeneous or fluorescently labeled neural cell populations are necessary.

Experimental procedures

Maintenance of human ESC and iPSC lines

Human embryonic stem cell line H13 was obtained from the Harvard Stem Cell Institute; the generation and characterization of the human induced pluripotent stem cell line NAS2 is described elsewhere (Devine et al., 2011). Human ESCs and iPSCs were expanded on irradiated CF1 MEFs (GlobalStem), in WiCell medium containing advanced DMEM/F12 (Life technologies), 10% KnockOut Serum Replacement (Life technologies), 2 mM L-glutamine (Life technologies), 1% non-essential amino acids (Millipore) and 50 μM β-mercaptoethanol (Sigma-Aldrich), supplemented with 20 ng/ml FGF2 (from Preprotech or Life Technologies). At thaw, in order to increase the yield of recovery of the colonies, 20 μM of the Rho-Kinase inhibitor Y-27632 (Abcam) was added to the medium. Medium was changed daily, and colonies were regularly passaged using dispase (Life Technologies). Cells were kept at 37 °C under 5% CO_2. The use of human ESCs and iPSCs is in line with Lund University and national guidelines.

cDNA construct

The pBluescript-Gfa_{ABC1D} was a gift from Prof. Michael Brenner (University of Alabama-Birmingham, USA). The construct encodes a 681 bp fragment of the human GFAP promoter that is sufficient to result in selective expression in murine astrocytes throughout the CNS (Lee et al., 2008). The full sequence of the fragment is provided in supplementary Fig. 1. The PGK::Neo-Hb9::GFP plasmid was a gift from Prof. Hynek Wichterle (Columbia University of New York, USA), and was previously used to generate a hESC line reporting on motor neurons (Di Giorgio et al., 2008). The GFA_{ABC1D} promoter fragment was inserted in place of the Hb9 promoter using Sal1 and Asc1 restriction sites. Then, the tRFP was inserted in place of the GFP using Asc1 and NheI restriction sites. The PGK::Neo-GFA_{ABC1D}::tRFP construct was checked by restriction and sequencing.

Generation of human ESC and iPS cell reporter lines

Nucleofection, selection and pre-screening were performed as follows: briefly, colonies of each single cell line (H13 and NAS2) were dissociated into single cell cultures, concentrated and electroporated (AMAXA, B-016 program) with the linearized vector (linearized using Not1 single restriction site). Nucleofected cells were seeded and grown on a monolayer of irradiated $CF6Neo^R$ MEFs (Globalstem) in WiCell medium supplemented with 20 μM Y-27632 and 20 ng/ml FGF2. Once colonies were formed, selection was applied by adding increasing concentrations of G418 (Life Technologies) to the medium. Every 3 days, G418 concentrations were increased two-fold, to a final concentration of 400 μg/ml. Resistant colonies were picked and expanded separately for storage and pre-screening. Here, cultures were considered positive once RFP expression was observed. Pre-screening was carried out using the midbrain differentiation protocol described hereafter.

Differentiation of human ESCs and iPSCs into CNS regionalized astrocytes

One day prior to start of differentiation, human ESC and iPSC colonies (wild-type or transgenic) were harvested using dispase, and seeded into ultra-low attachment plates (Corning) in Wicell medium supplemented with FGF2 and Y-27632. The day after (day 0), patterning of newly formed embryoid bodies (EBs) toward midbrain (floor-plate) or spinal cord fate was initiated. For patterning into midbrain identity, medium was changed to advanced DMEM/F12:Neurobasal (1:1) supplemented with 2% (v/v) B27 minus vitamin A and 1% (v/v) N2, 2 mM L-glutamine, 1% non-essential amino acids and penicillin/streptomycin (all from Life Technologies). Midbrain identity was directed by supplementing media with 0.1 μM LDN-193189 (from D0 to D8; Stemgent), 10 μM SB-431542 (from D0 to D6; Sigma-Aldrich), 200 ng/ml SHH-C25II N-terminus (from D0 to D12; Life Technologies), 0.8 μM CHIR-99021 (from D0 to D12; Stemgent) and 1 μM of smoothened agonist (SAG; from D2 to D12; Millipore), as previously described (Kirkeby et al., 2012a). Medium was changed every other day. Patterning toward spinal cord lineage was started in WiCell media (from D0 to D4) with a gradual shift (from D4 to D6) to glial induction media (GIM) composed of advanced DMEM/F12 with 2% (v/v) B27 plus vitamin A, 2 mM L-glutamine, 1% (v/v) non-essential amino acids and penicillin/streptomycin. Media were supplemented with 0.1 μM LDN-193189 (from D0 to D6) and 10 μM SB-431542 (from D0 to D6), 1 μM of retinoic acid (RA; from D2 to D12, Sigma-Aldrich), 200 ng/ml SHH-C25II N-terminus (from D6 to D12), 10 ng/ml BDNF (from D6 to D12, Life Technologies), 0.4 μg/ml ascorbic acid (from D6 to D12, Sigma-Aldrich), as recently described (Lamas et al., 2014). For both midbrain and spinal patterning, medium was changed every other day. From day 12 of differentiation, free-floating cultures containing regionalized EBs were grown in GIM supplemented with 20 ng/ml FGF2 and 100 ng/ml EGF (Preprotech; Nelson et al., 2008). EBs were cultured under these conditions until day 45 and medium was changed twice a week. At day 45, EBs were collected and dissociated using Accutase (Life Technologies).

Single cells were then seeded on 20 ng/ml poly-ornithine (Sigma-Aldrich) and 5 μg/ml laminin (Life Technologies). Cells were cultured in GIM supplemented with 1% (v/v) FBS (Life Technologies) until day 130. When confluent, cultures were passaged using trypsin-EDTA (Life Technologies).

Flow cytometry analysis and FACS

Cells were dissociated using trypsin and re-suspended in magnesium/calcium-free PBS supplemented with 10% FBS (v/v). Samples were analyzed and sorted using a BD FACSAria III (BD Biosciences) with FACSDiva v8.0 software (BD Biosciences), at the MultiPark Cellomics and Flow Cytometry Core technical platform, at Lund University. The cytometer was set up using a 100 μm nozzle at standard pressure of 20 psi and a frequency of 30.0 kHz and was calibrated daily using BD FACSDiva Cytometer Setup and Tracking (CS&T) software and CS&T Research Beads (BD Biosciences). For sorting, drop delay was optimized with Accudrop beads (BD Biosciences) to >99% of beads sorted in "fine tune" sort mode. Cells were sorted at sort mode 0-32-0 (yield mask 0, purity mask 32, phase mask 0). 7-Aminoactinomycin D (7AAD) was excited by the blue laser (488 nm/20 mW) and emission was detected through a 695/40 bandpass (BP) filter. RFP was excited by the yellow/green laser (561 nm/50 mW); emission at 610/20 BP. PMT were set using unstained and fully stained cells and emission was detected as the area of fluorescence intensity. In short, the strategy for gating was separating out 1) single cells based on FSC-W/FSC-A and SSC-W/SSC-A (Supplementary Fig. 2A and B), 2) live and dead cells based on uptake of 7AAD (Supplementary Fig. 2C), and 3) RFP positive cells compared to non-reporter expressing astrocytes (Supplementary Fig. 2D). Compensation was set up using single-positive cells for RFP and 7AAD. Each analysis was based on 10,000 to 20,000 events. Samples were sorted at 4 °C directly into GIM medium supplemented with 1% (v/v) FBS. Re-analysis of test-samples showed sort purity greater than 97% and dead cells <5% of non-enriched populations. Sorted cells were then seeded onto poly-ornithine/laminin-coated plates.

Immunocytochemistry

Cells were fixed using 4% paraformaldehyde (Sigma-aldrich) for 30 min at room temperature and incubated for 1 h at room temperature (RT) with blocking buffer containing 0.1% Triton-X (Sigma-Aldrich) and 10% donkey serum (Millipore) in PBS. Subsequently, cells were incubated with primary antibodies diluted in blocking buffer overnight at 4 °C. Cultures were then washed with PBS and incubated with secondary antibodies in PBS 0.1% Triton-X for 1 h at RT. Primary antibodies used in this study were: polyclonal anti-GFAP (1:5000; Z033401-2, DAKO), monoclonal anti-GFAP (1:100; G3893, Sigma-Aldrich), monoclonal anti-HOXB4 (1:80; I12 anti-Hoxb4, DSHB), polyclonal anti-OTX2 (1:500; AF1979, R&D), polyclonal anti-GLAST (1:200; AF6048, R&D), monoclonal anti-Glutamine synthetase (1:1000; MAB302, clone GS-6, Millipore), monoclonal anti-CD44-FITC (1:30; 555478, clone G44-26, BD-Bioscience), polyclonal anti-LMX1A (1:500; 50.5G5, DSHB), monoclonal anti-FOXA2 (1:100; sc-6554, Santa Cruz Biotechnology), polyclonal anti-NF1A (1:100; 39036, Active Motif), monoclonal anti-S100β (1:500; S2532, Sigma-Aldrich), monoclonal anti-CX43 (1:500; C6219, Sigma-Aldrich), polyclonal anti-tRFP (1:5000; AB234, Evrogen). For fluorescence microscopy analysis, secondary antibodies conjugated to Alexa-488, 555 or 647 (1:400; Donkey, Life Technologies) were used.

RT-qPCR

Cultures of progenitors aged 12 DIV were treated with Trizol for RNA extraction, according to standard procedures. Samples were analyzed using the Bio-Rad CFX-96 apparatus, using a protocol customized according to the instructions of the SsoFast™ EvaGreen® Supermix (Bio-Rad). Relative quantification was applied using the GAPDH as reference gene. All RT-qPCR reagents were purchased from Life Technologies. The following primers were used: EN1, GTGTCTGCCCACCTCT TCTC (For) and GCAGTCTGTGGGGTCGTATT (Rev); FOXA2, CC GTTCTCCATCAACAACCT (For) and GGGGTAGTGCATCACCTGTT (Rev); GAPDH, GAAATCCCATCACCATCTTCCAGG (For) and GAGCCCCAGCCTTCTCCATG (Rev); HOXB4, ACACCCGCTAACAA ATGAGG (For) and GCACGAAAGATGAGGGAGAG (Rev); LMX1A, AGAGCTCGCCTACCAGGTC (For) and GAAGGAGGCCGAGGTGTC (Rev); OTX2, GAAGCTCCATATCCCTGGGTGGAAAG (For) and CCATGACCTATACTCAGGCTTCAGG (Rev); PAX6, GGCAACCTAC GCAAGATGGC (For) and TGAGGGCTGTGTCTGTTCGG (Rev).

Microscopy and quantification

Cultures were imaged under an inverted microscope (Olympus IX73 equipped with Hamamatsu C11440 Orcaflash 2.8 camera). Whole well images were acquired using the plate Runner HD from Trophos (at a resolution of 2046 × 2046 pixels). Automated quantitative image analysis of fluorescent and stained astrocyte cultures was performed using the MetaMorph Software V7.8.6.0 (Molecular Devices). Quantitative analysis of stained hPSC-derived astrocyte cultures was performed using the Multi-Wavelength Cell Scoring application. For a specific marker, positive cells were selectively identified as having clear signal intensity above local background. Intensity thresholds were set blinded to sample identity. In a given experiment the same parameters were used in all images analyzed, for all conditions. Parameters were only minimally adjusted across different experiments.

IL-6 ELISA and protein array

FACS-purified astrocytes were seeded in GIM medium containing 1% (v/v) FBS 2 days before the experiment. On the day of the experiment cells were washed twice with non-supplemented GIM and subsequently treated with either GIM plus 1% (v/v) FBS or GIM pus 10 ng/ml IL-1β (R&D). On day 7, media was harvested for protein array and ELISA. Briefly, for ELISA analysis samples were diluted 1:10 and applied to an IL-6 ELISA assay (KHC0061, Life Technologies), according to manufacturer's guidelines. Absorbance at 450 nm was measured by spectrophotometry. Human cytokine array panel A (ARY005, R&D Systems) was used according to manufacturer's guidelines. Intensities were measured using ChemiDoc software (Bio-Rad) and were normalized to mean intensities of reference spots.

Preparation of aSYN species and treatment of astrocyte cultures

Human alpha-synuclein (S 1001 2, rPeptide) was Atto-labeled according to the manufacturer protocol (#38371 Sigma). Fibrils were generated by mixing 100 μg of human alpha-synuclein and 21 μg of Atto-labeled human alpha-synuclein in a total volume of 165 μl 50 mM Tris, 250 mM NaCl, pH 7.5 solution. This solution was incubated for 7 days at 37 °C (in the dark) using the following cycle: Shaking (300 rpm) 3 days, left overnight without shaking, shaking for 4 additional days. Preparations were then evaluated by electron microscopy to ensure that fibrillation had taken place (data not shown). Before use, fibrils were sonicated twice 30 s at 40% amplitude with a sonicator (QSonica, 125A-220). Cultures were then incubated with 0.7 μM of either monomers or fibrils for the indicated periods.

Results

Astrocyte differentiation varies significantly between midbrain, but not spinal cord, cultures

Our overall aim was to generate fluorescence-based PSC reporter lines for the isolation of and reporting on human astrocytes generated from regionally distinct neural progenitors. Since human ESC are most commonly utilized to generate reporter lines (Di Giorgio et al., 2008; Fischer et al., 2010; Liu et al., 2011; Placantonakis et al., 2009) we used the human ESC line, HuES13 (H13) for generating our astrocyte reporter line. At first, we developed neural induction protocols that specify neuroepithelial cells toward ventral spinal cord or ventral midbrain floor-plate identities. For the rapid generation of regionalized progenitors, human ESCs were routinely expanded as adherent colonies on irradiated MEFs, and dissociated and seeded onto Matrigel-coated plates forming monolayer cultures. When confluent, cultures were neuralized by dual inhibition of SMAD signaling using LDN and SB (Chambers et al., 2009), and regionalized toward a caudal ventral fate or midbrain ventral fate using RA and SHH or CHIR and SHH and SAG, respectively (Fig. 1A), as previously described (Kirkeby et al., 2012b; Krencik et al., 2011; Kriks et al., 2011; Roybon et al., 2013). We monitored the appearance of regional identity markers 12 days after initial treatment with the patterning factors. Neural progenitors directed toward a caudal ventral fate expressed HOXB4 and FOXA2, while those directed toward a midbrain ventral fate expressed FOXA2 and lacked HOXB4. Notably, midbrain neural progenitors co-expressed FOXA2 and LMX1A (Fig. 1B and C). Because we employed low concentrations of SHH (200 ng/ml), few LMX1A-expressing cells could be detected in spinal cord cultures. These LMX1A positive cells however were negative for FOXA2, and were representative of a more dorsally located population in the spinal cord (Chizhikov and Millen, 2004). The majority of the cells expressing FOXA2 were reminiscent of populations located more ventrally (Lek et al., 2010; Ribes et al., 2010). We confirmed the regional identity of the neural progenitors by RT-qPCR for the markers OTX2, EN1, LMX1A, FOXA2, HOXB4 and PAX6 (Fig. 1E). Thus, treatment with LDN, SB, RA and SHH (hereafter referred to as the spinal protocol) mainly resulted in the production of FOXA2$^+$/PAX6$^+$/HOXB4$^+$ neural progenitors, while treatment with LDN, SB, CHIR and SHH (hereafter referred to as the midbrain protocol) resulted in cultures containing OTX2$^+$ midbrain floor plate neural progenitors co-expressing FOXA2 and LMX1A.

We next expanded the neural progenitors in medium containing FGF2 and EGF to generate cultures enriched in glial progenitors (Krencik et al., 2011), which we differentiated into astrocytes by withdrawal of the mitogens, and adding FBS (Roybon et al., 2013) (Fig. 1A). Three months after the initiation of the spinal cord and midbrain differentiations, we could still identify the presence of regional identity markers HOXB4 and OTX2, in spinal cord and midbrain cultures, respectively (Fig. 1D). Notably, we observed a robust expression of GFAP in spinal cord cultures (Fig. 1F). This was however not the case for midbrain cultures (Fig. 1G). Out of 10 midbrain cultures differentiated from ESC stage, half gave rise to large amounts of GFAP-expressing cells, while all spinal cord cultures robustly generated GFAP-expressing cells (hereafter referred to as spinal cord astrocytes). The variability in GFAP-expressing astrocytes generated from human ESC-derived midbrain progenitors (hereafter referred to as midbrain astrocytes) may indicate that the purity of neural progenitors in midbrain cultures is not always ascertained, or that the degree of maturity of midbrain astrocytes in cultures may differ between preparations. This result emphasized the need for generating cellular models that would enable identification and/or purification of astrocytes for several purposes.

Methodology for generating stable transgenic hESC lines reporting on astrocyte differentiation

Several methods exist to generate fluorescence-based reporter cell lines. The most commonly employed are BAC transgenesis (Placantonakis et al., 2009; Rostovskaya et al., 2012) and gene targeting (Fischer et al., 2010; Liu et al., 2011), but those require large plasmids which often break during electroporation and specific molecular tools not always accessible in every laboratory, respectively. Here, we generated stable human ESC lines by electroporation of a plasmid containing a neomycin resistance gene and a red fluorescent protein gene which are driven by the phosphoglycerate kinase-1 promoter and the ABC1D region of the human *GFAP* promoter, respectively (Fig. 2A and Supplementary Fig. 1; see Experimental procedures). Colonies surviving geneticin (G418) selection (n = 39) were harvested and individually expanded for differentiation and cryopreservation (Fig. 2B). Although the selected clones carried the resistance cassette, it is possible that the reporter cassette, despite its small size, was damaged during electroporation. Therefore, we performed a second selection by pre-screening the resistant clones for reporter expression. Since variability was observed in the amount of GFAP-expressing cells generated using the midbrain protocol, but not the spinal protocol, we decided to differentiate the clones using the midbrain protocol at first, to ensure the selection of TagRFP-expressing clones, in advance of extended characterization and validation using the spinal cord protocol. We differentiated the 39 neomycin-resistant clones into midbrain astrocytes as adherent cultures

in a 96 well plate format and observed for reporter expression. When most of the cultures reached confluence, all differentiating clones were simultaneously passaged. After 70 days of *in vitro* culture, natural fluorescence-based reporter expression was assessed. Twelve of the 39 clones showed reporter expression and immunohistochemistry revealed co-localization of TagRFP with GFAP in 11 clones (Fig. 2C). Thus, these two steps of selection allowed identification of 11

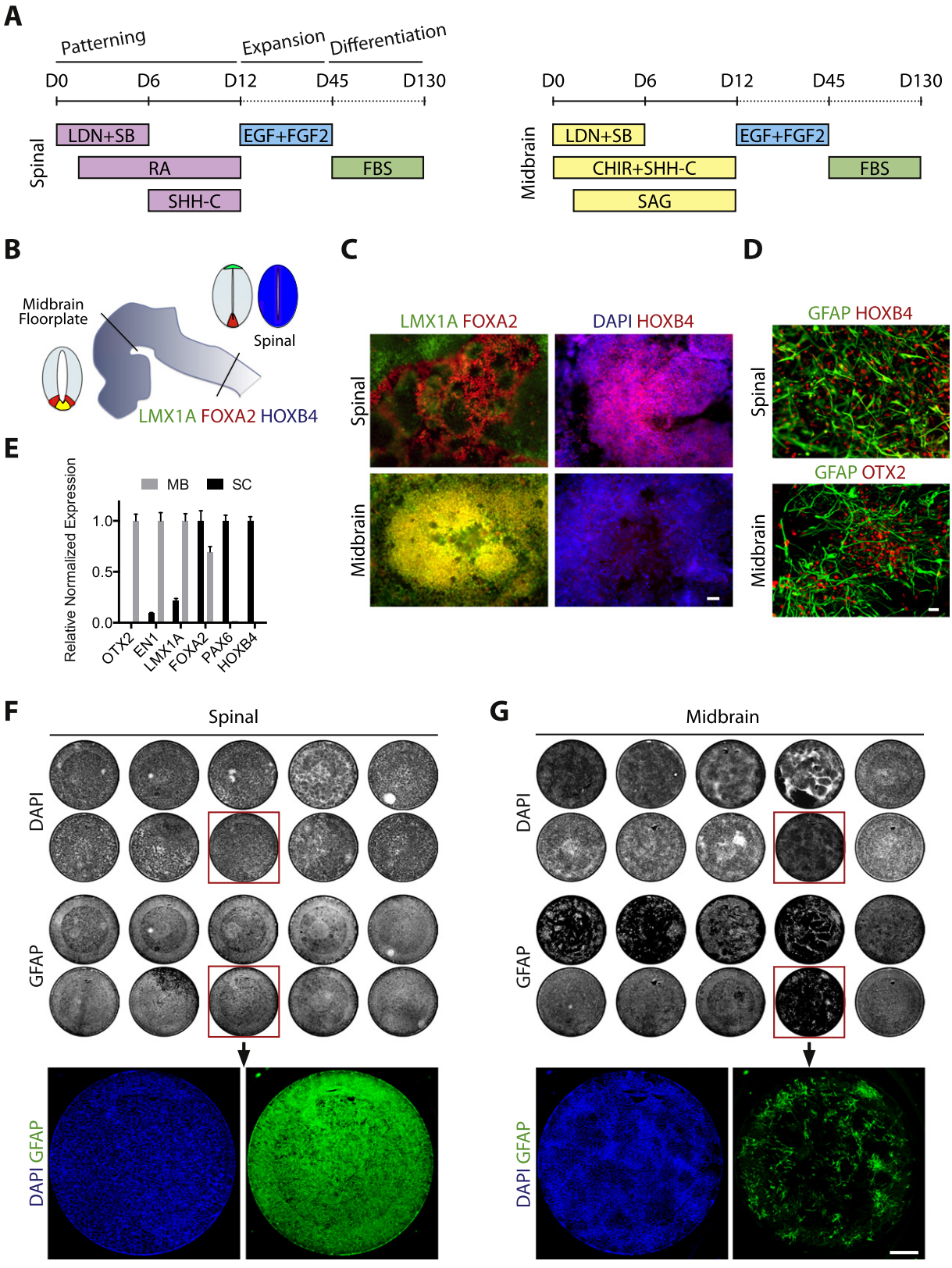

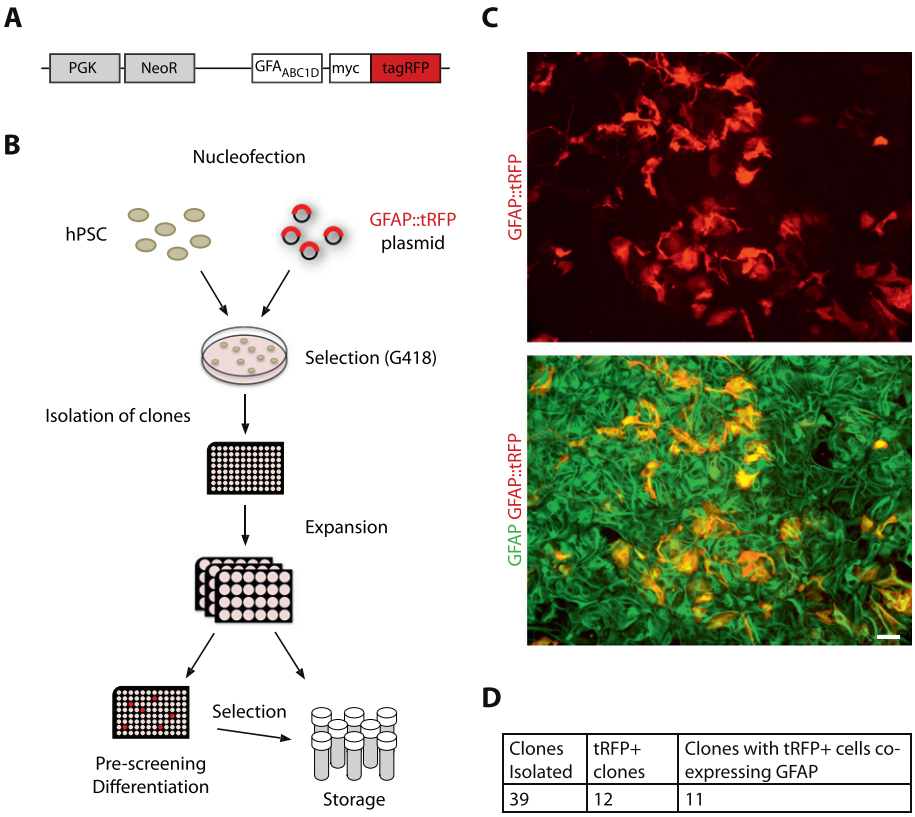

Clones Isolated	tRFP+ clones	Clones with tRFP+ cells co-expressing GFAP
39	12	11

Figure 2 Generation of astrocyte reporter lines from hESC. A. Schematic representation of the construct generated and used to generate astrocyte pluripotent stem cell reporter lines. B. Strategy employed for generating astrocyte reporter lines from human embryonic stem cells. Nucleofection of reporter construct into PSCs followed by selection for resistant clones using geneticin. After expansion of the clones pre-screening was preformed for selection of clones co-expressing GFAP and *GFA$_{ABC1D}$::TagRFP*. C. Detection of reporter expression in cultures aged 70 DIV, during the pre-selection phase. Images show abundance of GFAP/*GFA$_{ABC1D}$::TagRFP*-cells. Scale bar represents 20 μm. D. Summary of the number of clones obtained during the different selection steps.

G418-resistant *GFA$_{ABC1D}$::TagRFP*-expressing clones (Fig. 2D); these were processed further to assess long-term reporter expression in astrocyte cultures.

Characterization of reporter expression in midbrain progenitor-derived astrocytes

We next characterized long-term reporter expression through a time course study of 130 days *in vitro* (DIV). Cultures were grown side-by-side, as free-floating embryoid bodies (EBs), in a 12 well-plate format (see experimental procedures). From day 45 onward, cultures were grown on adherent substrate in medium containing FBS (1% v/v) to allow differentiation of midbrain neural precursors into astrocytes. At this stage of differentiation, attached cultures were passaged weekly and cells were harvested for analysis of reporter expression using FACS at 70, 90, 110 and 130 days of differentiation *in vitro* (Fig. 3A and Supplementary Fig. 2). We could not detect *GFA$_{ABC1D}$::TagRFP* in EBs (data not shown) and cultures of midbrain progenitors aged 45 DIV (Fig. 3B). This was not the case in older cultures where differences were clearly identified between clones, in term of intensity of reporter expression and number of cells expressing *GFA$_{ABC1D}$::TagRFP*

Figure 1 Differentiation of hESC-derived ventral spinal cord and ventral midbrain progenitors into GFAP-expressing astrocytes. A. Schematic representation of the protocols used to differentiate hESCs into ventral spinal cord and ventral midbrain progenitors and subsequent differentiation into astrocytes. B. Overview of the location of and protein expression in spinal and midbrain floor-plate regions of the neural tube. C. Immunocytochemistry performed at day 12 of differentiation reveals co-expression of LMX1A and FOXA2, and absence of HOXB4 in ventral midbrain progenitors. Spinal cord progenitors express HOXB4 and do not co-express LMX1A and FOXA2. Scale bar represents 50 μm. Images are representative of more than five differentiations. D. Immunocytochemistry performed at day 70 of differentiation shows abundance of regionally specified cells in midbrain and spinal cord cultures expressing OTX2 and HOXB4, respectively. Images are representative of n = 2 differentiations. Scale bar represents 20 μm. E. RT-qPCR analysis shows up-regulation of regional identity markers in cultures differentiated toward midbrain floor plate and ventral spinal cord lineages. Mean ± s.e.m.; n = 3. F and G. Images of whole culture wells stained for GFAP (green) and DAPI (blue) at day 90 of differentiation reveals variability in the amount of GFAP-expressing cells produced for 10 midbrain differentiations started side-by-side from pluripotent stem cell stage. Scale bar represents 1 mm.

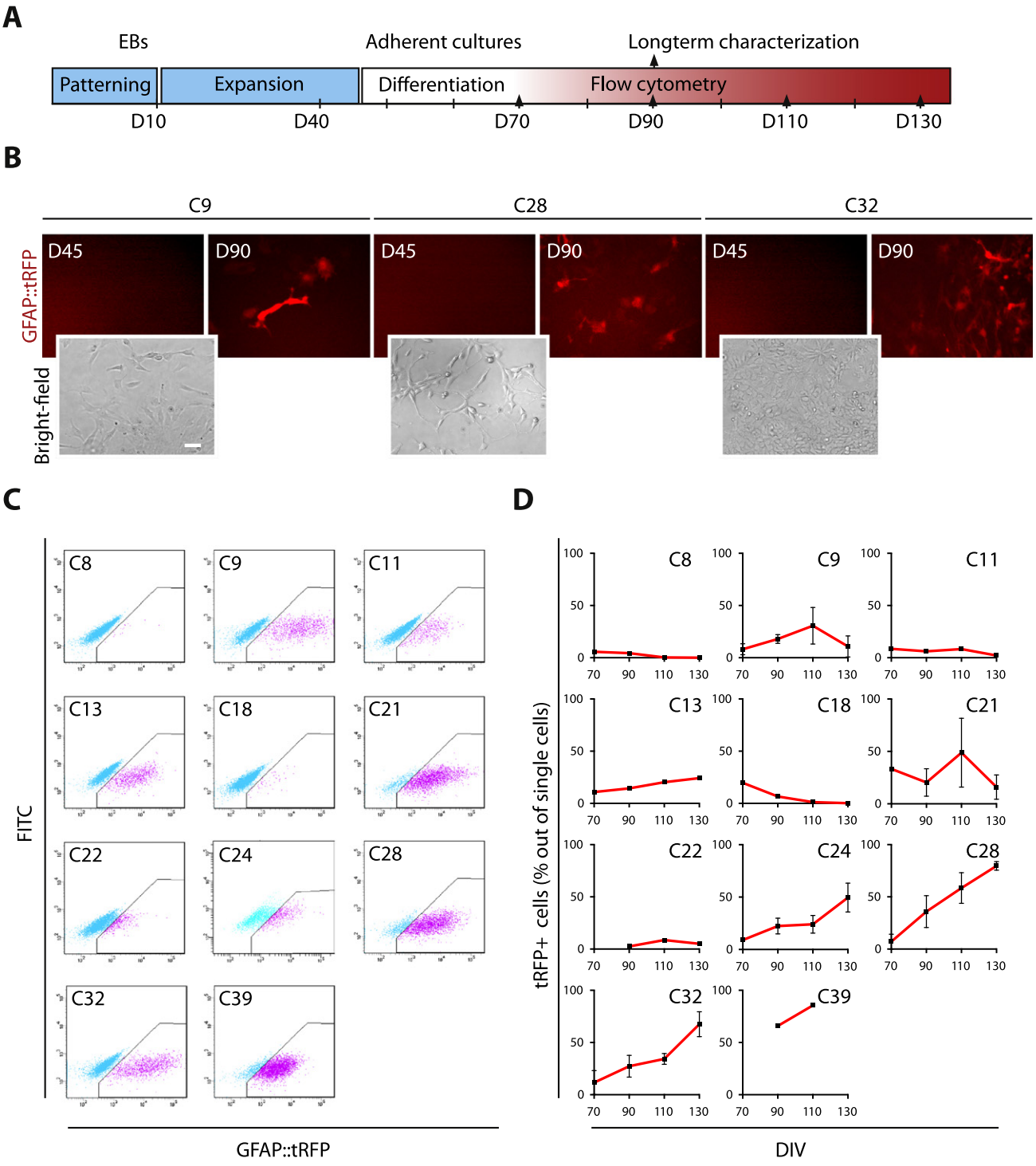

Figure 3 Characterization of reporter expression in midbrain progenitor-derived astrocytes, *in vitro*. A. Schematic representation of the experimental approach carried out to study reporter expression. Cultures were grown on adherent substrate from day 45 onward, and passaged at confluency. Lower black arrows represent the time points for flow cytometry analysis. Upper black arrow represents FACS purification of cultures for long-term characterization. B. Absence of reporter expression in adherent cultures at 45 DIV. Cells express the reporter after 90 DIV. Inset show bright-field images of cultures devoid of *GFA*$_{BC1D}$*::TagRFP*-expressing cells. Scale bar represents 20 μm. C. Flow cytometry plots represent live single cells analyzed for reporter expression, at day 110 of differentiation, and reveal differences in reporter intensity and number of *GFA*$_{BC1D}$*::TagRFP*-expressing cells. D. Graphs represent time course study of the percent of *GFA*$_{ABC1D}$*::TagRFP* positive cells out of live single cells, measured by flow cytometry. Missing values are the result of insufficient cells for FACS analysis due to slow division rate (C22 and C39, day 70), or loss of cells due to bacterial infections (C39, day 130). Mean ± s.e.m.; n = 3 differentiations.

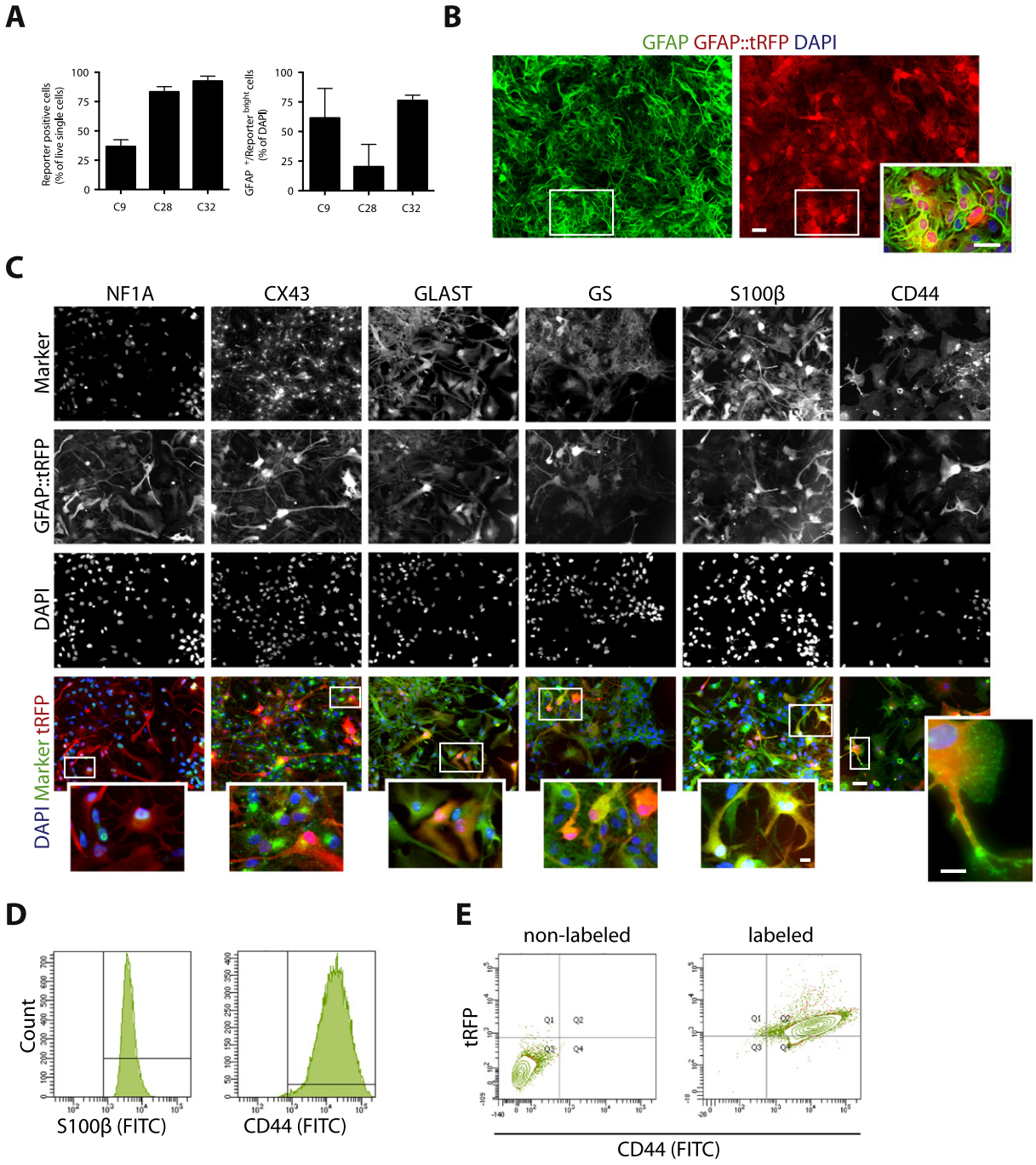

Figure 4 Long-term characterization of FACS-purified cultures, using the midbrain astrocyte protocol. A. Reporter and GFAP expression assessed for C9, C28 and C32 in purified cultures, at 130 DIV. Bar diagrams represent the percentage of *GFA$_{ABC1D}$::TagRFP* positive cells (out of living cells; measured by FACS) and the percentage of GFAP/*GFA$_{ABC1D}$::TagRFP^{bright}* double positive cells (out of DAPI stained cells). Mean ± s.e.m.; n = 3 separate differentiations. B. Maintenance of reporter expression (red) in purified C32 midbrain cultures coincides with GFAP (green) expression. Scale bar represents 20 μm. C. Panel of canonical markers expressed by midbrain astrocyte 40 days post-enrichment by FACS; at this time point, cultures are 130 DIV. Images show homogenous cultures of astrocytes co-expressing TagRFP and canonical markers NF1A, CX43, GLAST, GS, S100β and CD44. Nuclei are indicated with DAPI staining. Scale bar in main panel represents 20 μm and in insets 5 μm (bottom right panels). D. Flow cytometry analysis of cultures stained for S100β or CD44 confirming the immunocytochemistry data. FACS plots show number of FITC-positive cells above threshold. E. Flow cytometry analysis of CD44 stained astrocytes. Left plot shows analysis of unstained astrocytes generated from a non-astrocyte report line (=non labeled control sample). Right plot shows TagRFP-expressing astrocytes co-expressing CD44 (shown for clone 32).

(Fig. 3B and C). Notably, FACS analysis of clones revealed that at 70 DIV, less than 25% of live single cells expressed *GFA$_{ABC1D}$::TagRFP* (Fig. 3D).

We next analyzed the degree of enrichment in *GFA-$_{ABC1D}$::TagRFP*-expressing cells after purification by FACS, and reporter expression after subsequent culture for a

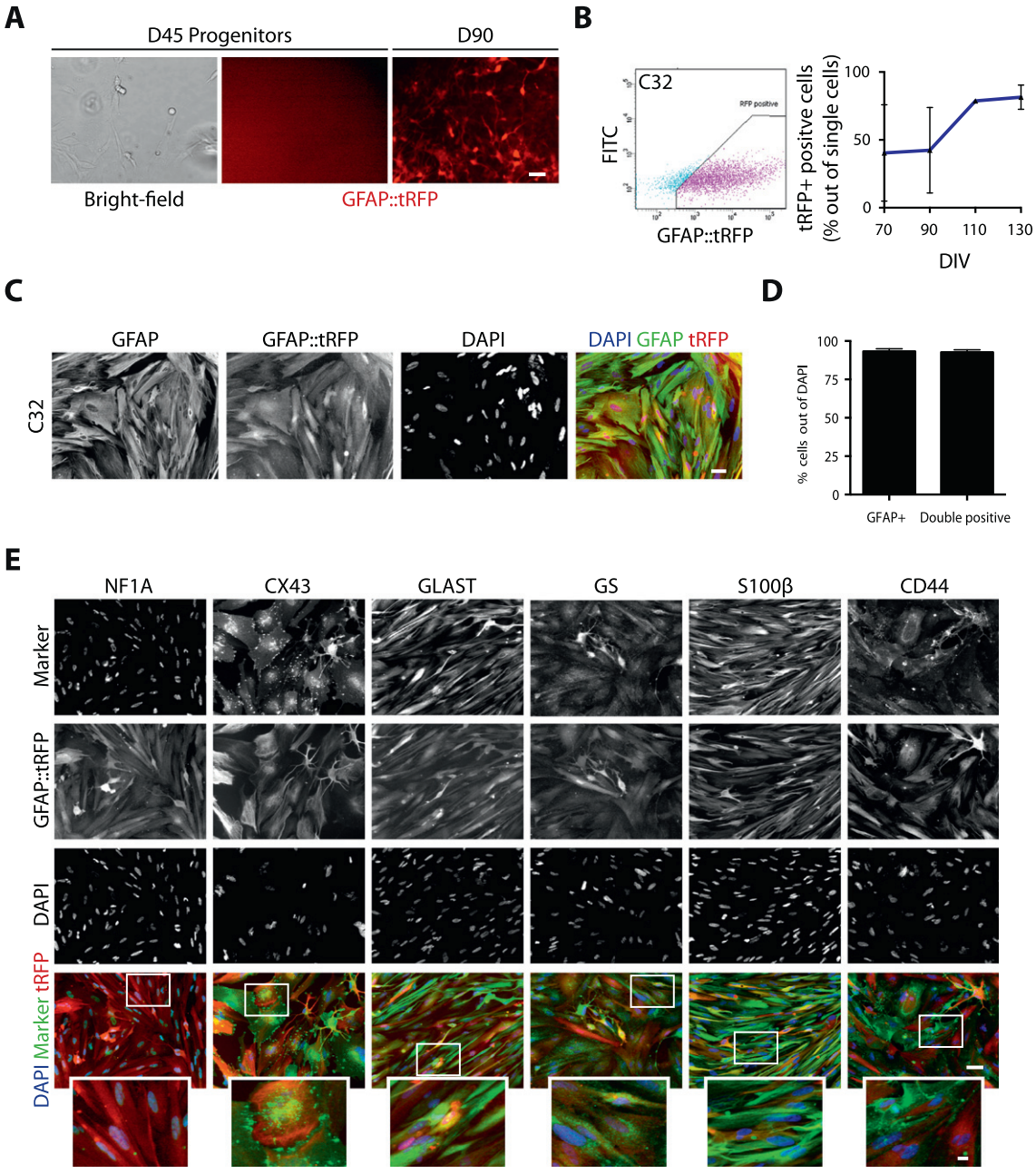

Figure 5 Long-term characterization of reporter expression in hESC transgenic clone C32, during differentiation of spinal progenitors into astrocytes. A. Absence and presence of reporter expression in spinal cultures at 45 DIV and 90 DIV, respectively. Bright-field image confirm the presence of cells in cultures aged 45 DIV. Scale bar represents 20 μm. B. FACS plot (on the left) shows live single cells analyzed for reporter expression, at day 110 of differentiation. The graph shows increase in the number of *GFA$_{ABC1D}$::TagRFP* positive cells out of live single cells, over time (measured by flow cytometry). Mean ± s.e.m.; n = 3 separate differentiations. C. Purified C32 spinal cord astrocytes grown for 40 additional DIV maintain tagRFP expression and co-express GFAP (green). Scale bar represents 20 μm. Nuclei are stained with DAPI (blue). D. Bar diagram show the total number of TagRFP-expressing cells (measured by FACS) and number of GFAP/TagRFP double positive cells in cultures purified at day 90, grown for 40 additional days, out of single cells. E. Panel of canonical markers expressed by spinal cord astrocyte in cultures, 40 days post-enrichment. Cultures are homogenous, and composed of TagRFP astrocytes co-expressing canonical markers NF1A, CX43, GLAST, GS, S100β and CD44. Nuclei are indicated with DAPI staining (blue). Scale bar in main panel represent 20 μm and in insets 5 μm.

period of 40 additional DIV, the latter to assess possible loss of reporter expression. For this analysis, we chose to characterize three clones: C9 and C32 which displayed strong reporter intensity measured by FACS, and clone 28 which gave rise to the greatest number of *GFA$_{ABC1D}$::TagRFP*-expressing cells, over time (Fig. 3D). Cultures FACS-purified on day 90, and grown for 3 additional days, showed a nearly complete enrichment in reporter-expressing cells (Supplementary Fig. 3A). This was however not observed in populations that were sorted after 90 DIV and subsequently cultured for 40 additional DIV. At that time point, assessment of reporter expression by FACS revealed a decrease in the number of *GFA$_{ABC1D}$::TagRFP*-expressing cells in purified culture for C9, whereas little change was observed in purified cultures for C28 and C32 (Fig. 4A). As the intensity of reporter expression varied between the clones, we next analyzed the overlap between GFAP and *GFA$_{ABC1D}$::TagRFP*. We performed quantitative analysis of bright fluorescent reporter (*GFA$_{ABC1D}$::TagRFP^{bright}*)-expressing cells in cultures stained for GFAP and DAPI. The percentage of cells co-expressing GFAP and *GFA$_{ABC1D}$::TagRFP^{bright}* for purified cultures of C32 reached ~80% of the GFAP-expressing cells. This however was not the case for C9 and C28 since the majority of the cells variably and weakly expressed the reporter. Thus, C32 appeared to be the most robust candidate clone suitable for reporting on midbrain astrocyte differentiation based on the co-expression of GFAP and *GFA$_{ABC1D}$::TagRFP^{bright}* (Fig. 4B).

The astrocyte identity of reporter-based purified C32 cells had yet to be validated using additional markers. We therefore performed immunocytochemistry on 130 DIV old C32 purified cultures, for the astrocyte markers NF1A, CX43, GLAST, GS, S100β and CD44 markers. While nearly all cells present in purified cultures at 130 DIV expressed the astrocyte markers (Fig. 4C), none stained positive for the neuronal and oligodendroglial markers neurofilament and CNPase, respectively (data not shown). FACS analysis of cultures stained for S100β or CD44 confirmed our immunocytochemistry data (Fig. 4D and E).

Characterization of reporter expression in C32 astrocyte cultures generated from hESC-derived spinal cord progenitors

Since we aimed to generate a stable transgenic hESC line reporting on astrocytes generated from midbrain and spinal progenitors from a single line, we repeated our analysis now on C32 astrocyte cultures generated using the spinal cord protocol. We differentiated clone C32 from hESC stage, as described above. As for midbrain cultures, spinal cultures contained cells with bright reporter expression (Fig. 5A and B) with a high degree of co-expression of GFAP and *GFA$_{ABC1D}$::TagRFP^{bright}*, 3 days after FACS (Supplementary Fig. 3B). Enrichment by means of FACS at day 90 and subsequent culture for 40 additional days resulted in homogenous cultures composed of GFAP/*GFA$_{ABC1D}$::TagRFP* expressing cells (Fig. 5C and D). At 130 DIV, nearly all purified cells present in culture expressed the astrocyte markers NF1A, CX43, GLAST, GS, S100β and CD44 (Fig. 5E).

Thus, clone C32 was selected as potential hESC line for the isolation of and reporting on astrocytes differentiated from midbrain and ventral spinal cord progenitors generated from a single hESC line.

Human ESC midbrain and spinal cord progenitor-derived GFA$_{ABC1D}$::TagRFP-expressing astrocytes are suitable for inflammatory profiling and protein uptake assays

The relevance of our cell models was tested using two distinct paradigms. The first consist of measuring the secretion of pro-inflammatory cytokines and chemokines from GFAP-expressing astrocytes only; it requires pure population of astrocytes in order to reach informative data, which could now be obtained by purifying astrocytes by FACS. The second assay consists of visualizing the uptake of labeled proteins, potentially pathogenic, into astrocytes; this assay requires that astrocytes are labeled and does not require homogenous cultures.

Purified midbrain and spinal cord astrocytes generated from C32 were treated for 7 days with FBS (1% v/v) or IL-1β (10 ng/ml; no FBS). IL-1β was shown to induce reactivity and expression and release of pro-inflammatory factors of hPSC-derived spinal cord astrocytes, which can be monitored by assessing the upregulation of the chemokine RANTES and the secretion of the cytokine IL-6 (Roybon et al., 2013). However, this had not been tested for astrocytes generated from hESC-derived ventral midbrain progenitors. Therefore, we performed a qualitative analysis using protein array, where we compared the changes in cytokine and chemokine secretions from FACS-purified astrocytes aged 130 DIV differentiated from midbrain and spinal cord neural progenitors from C32, following treatment with IL-1β (Fig. 6A). Protein array analysis showed that IL-6 was not released in FBS treated samples, in contrast to cultures treated with IL-1β, which is concordant with previous finding (Roybon et al., 2013). Similar levels of IL-6 secreted by the astrocytes were detected in both spinal and midbrain cultures; this lack of difference in IL-6 secretion between midbrain and spinal cord astrocytes was further confirmed by ELISA (data not shown).

Several other cytokines and chemokines were also newly secreted upon IL-1β treatment for both midbrain and spinal cord cultures (Fig. 6A). Interestingly, GROα (also known as CXCL1) and IL-8 were already present in midbrain cultures treated with FBS, while they were newly secreted in spinal cord cultures treated with IL-1β. In general, a tendency towards increasing secretion of similar chemokines and cytokines in both IL-1β-treated midbrain and spinal cord cultures was observed. The only drastic decline observed between treatments concerned CCL2 (also known as MCP-1), whose secretion was decreased following IL-1β treatment in both midbrain and spinal cord cultures (Fig. 6A). This finding is in line with recent work showing a down regulation of this protein in cultures composed of primary inflammatory human astrocytes (Choi et al., 2014), and whose absence exacerbates the release of several pro-inflammatory cytokines including IL-6, G-CSF, IL-1β and CXCL1, indicating a negative regulatory role of CCL2 in neuroinflammation (Semple et al., 2010). In general, no dramatic differences in cytokine and chemokine secretions were observed between midbrain and spinal cord cultures treated with IL-1β.

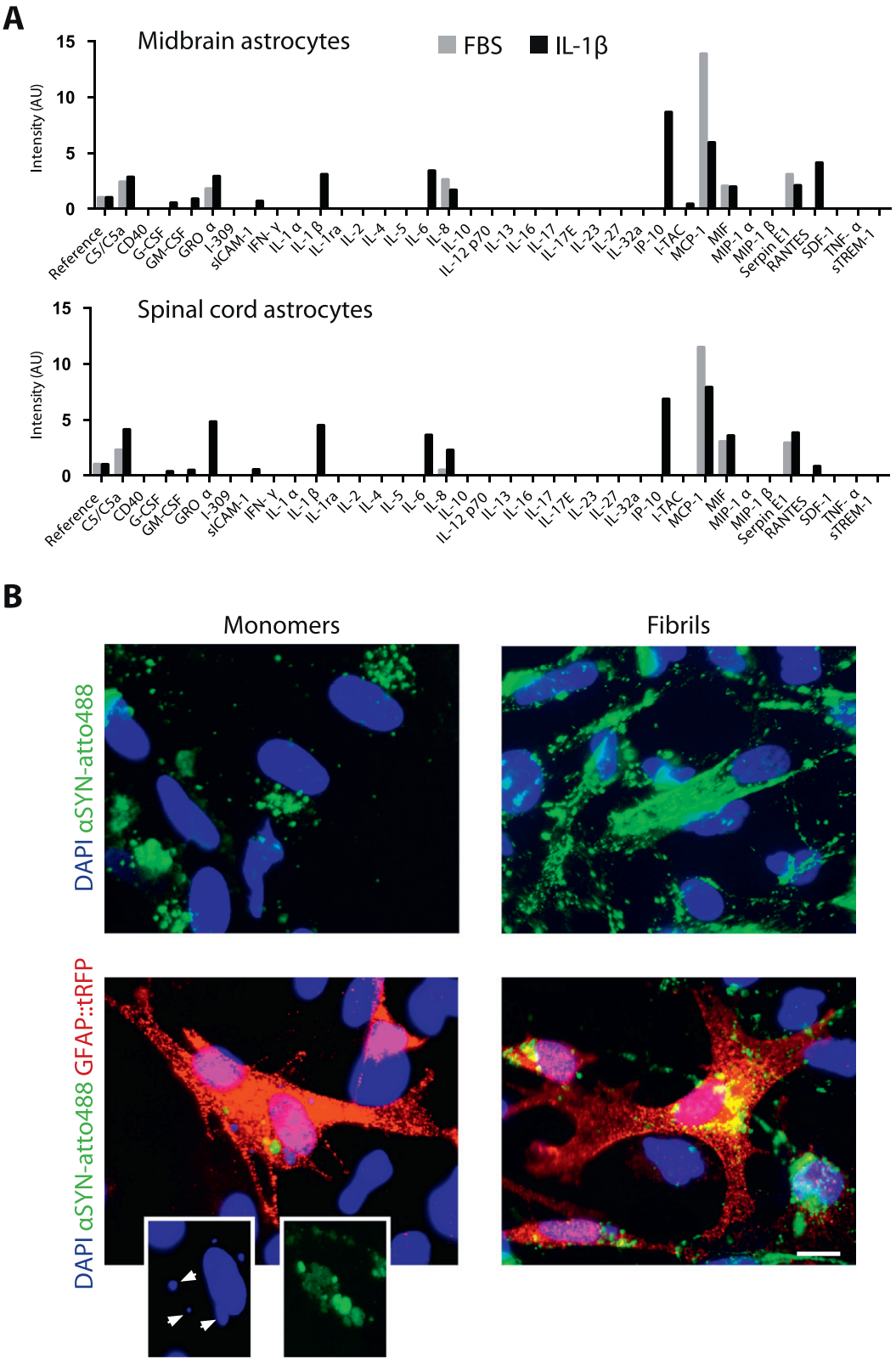

Figure 6 Examples of read-out assays using *GFA$_{ABC1D}$::TagRFP* astrocytes. A. Overview of the cytokines and chemokines expressed following treatment with FBS and IL-1β, of purified midbrain and spinal cord astrocytes aged 130 DIV. B. Upper panel images show cellular localization of αSYN in 90 DIV unpurified midbrain astrocyte cultures treated for 3 h with ATTO488-labeled αSYN species. Lower panel images show cellular localization of aSYN in cultures treated with ATTO488-labeled aSYN species, at 7 DIV. White arrowheads pinpoint DNA fragmentation. Scale bar represents 10 μm.

A large body of evidence suggests that glia play an important role in synucleinopathies through the accumulation of pathogenic proteins such as α-synuclein. Since rodent primary glia (astrocytes and microglia) can internalize α-synuclein *in vitro* (Lee et al., 2010; Zhang et al., 2005), and α-synuclein inclusion bodies were described in people with PD (Wakabayashi et al., 2000), we attempted to demonstrate additional relevance of our models, by investigating whether labeled α-synuclein protein could be tracked in *GFA$_{ABC1D}$::TagRFP*-expressing human astrocytes derived from midbrain progenitors. This test would further confirm the functionality of our astrocytes by being capable of taking up proteins. For this aim, we treated unpurified cultures generated from the clone C32 and aged 90 DIV, with ATTO488-labeled α-synuclein species. Three hours treatment sufficed to observe ATTO488-labeled α-synuclein monomers in vesicular-like structures in all cells. In contrast, fibril species seemed to accumulate at the cellular membrane (Fig. 6B), as recently observed by Reyes and coworkers, in an OLN-93 cell line model for oligodendrocytes treated with α-synuclein fibrils (Reyes et al., 2014). After 7 days of treatment, both monomers and fibrils were clearly observed in vesicular-like structures, demonstrating ongoing clearance of α-synuclein species by human astrocytes (Fig. 6C). Interestingly, we identified the presence of peri-nuclear inclusions and DNA fragmentation in *GFA$_{ABC1D}$::TagRFP*-expressing astrocytes, as previously described in other cellular experimental models (Bousset et al., 2013; Lee et al., 2010).

Overall, our data show that C32 can be used to generate homogeneous populations of functional astrocytes from regionally defined neural progenitors, which can be used for studies of inflammation *in vitro*, and to track the dynamics of pathogenic proteins in human fluorescently labeled astrocytes.

Generation of GFA$_{ABC1D}$::TagRFP report line for the reporting on astrocytes generated from human induced pluripotent stem cell-derived midbrain and spinal cord progenitors

Since human iPSCs are becoming an important model for investigating human diseases *in vitro* (Wichterle and Przedborski, 2010), we decided to test whether our strategy for generating hESC lines reporting on astrocytes could successfully be applied to hiPSCs. Similar to hESC, we generated hiPSC lines for reporting on midbrain and spinal cord astrocytes. We nucleofected the previously characterized hiPSC line, NAS2 (Devine et al., 2011), and harvested G418-resistant clones (n = 88) which we pre-screened using the methodology we described for the hESC clones. Out of 88 resistant clones, 14 clones showed reporter expression in cultures differentiated for 70 DIV, and co-expressed GFAP. These were selected and expanded for cryopreservation and further analysis. The clones were then differentiated from pluripotent stage using the protocols we developed to generate spinal cord and midbrain progenitors. At day 45 of differentiation, few cells in several clones differentiated using the astrocyte spinal cord protocol expressed the reporter (Fig. 7A). The number of reporter expressing cells increased over time similar to what was observed for the hESC clone C32 (Fig. 7B). Clone C70 was selected based upon live imaging and FACS analysis. Reporter-expressing cells in purified midbrain and spinal astrocyte cultures aged 130 DIV, both expressed NF1A, S100β and CD44 (Fig. 7C and D) as well as GLAST, GS, and CX43 (data not shown). Moreover, purified astrocytes were functional as they secreted IL-6 upon stimulation with IL-1β and it was possible to identify ATTO488 labeled α-synuclein in TagRFP astrocytes (Fig. 7E), similar to hESC-derived midbrain astrocytes. Therefore, we concluded that our protocol for generating human PSC reporter lines was also applicable to hiPSCs, and that the functional assays conducted using the reporter lines were relevant for both human ESC- and iPSC-derived astrocytes.

Discussion

Human astrocytes are highly heterogeneous and little is known about their development in the CNS. Differentiation of human PSCs into regionalized neural progenitors, which can be further differentiated into astrocytes, offers a new venue of research contributing to investigations of astrocyte development and diversity. These regionally specified astrocytes could be valuable models for studies of disease mechanisms, or as therapeutic vehicles, and homogeneous cultures of fluorescently labeled astrocytes could be an advantage over the use of heterogeneous, non-fluorescently labeled astrocytes for these purposes. Therefore, we engineered human PSC lines to report on astrocytes generated from regionally specified progenitors.

First, to enable investigation of the lines reporting on midbrain and spinal cord astrocytes, two differentiation protocols were developed. These rely on three different steps where neural progenitors are generated and regionalized, expanded and finally differentiated into astrocytes. The midbrain protocol led to the generation of PAX6$^-$/EN1$^+$/OTX2$^+$ midbrain floor-plate neural progenitors co-expressing LMX1A and FOXA2, while the spinal cord protocol led to the emergence of PAX6$^+$/FOXA2$^+$/HOXB4$^+$ caudal-ventral progenitors. Interestingly, GFAP expression largely varied between different cultures independently differentiated with the midbrain protocol, at day 90 of differentiation, while GFAP expression between spinal cord cultures was relatively similar. This difference might be attributable to the use of retinoic acid for generating spinal cord astrocytes. Indeed, retinoic acid is one of the most potent inducers of neural differentiation in human ESCs (Schuldiner et al., 2000). Moreover, protocols for generating spinal cord astrocytes have been more widely used, and are better optimized than the few developed for generating midbrain astrocytes. Thus, our new cellular models could help devise new protocols for the robust generation of human PSC-derived midbrain floor plate astrocytes, as well as protocols for generating astrocytes from other brain regions (e.g. dorsal and ventral forebrain astrocytes), provided that reporter expression is confirmed in cortical and striatal astrocytes.

We chose to use the human GFA$_{ABC1D}$ promoter to drive TagRFP in human astrocytes because of its accuracy to specifically direct reporter expression in astrocytes in several CNS regions, at embryonic and adult stage, in rodent (Lee et al., 2008). Interestingly, during the pre-screening stage, at 70 DIV, not all GFAP-expressing astrocytes co-expressed *GFAP::TagRFP* (Fig. 2C). This demonstrated that increasing

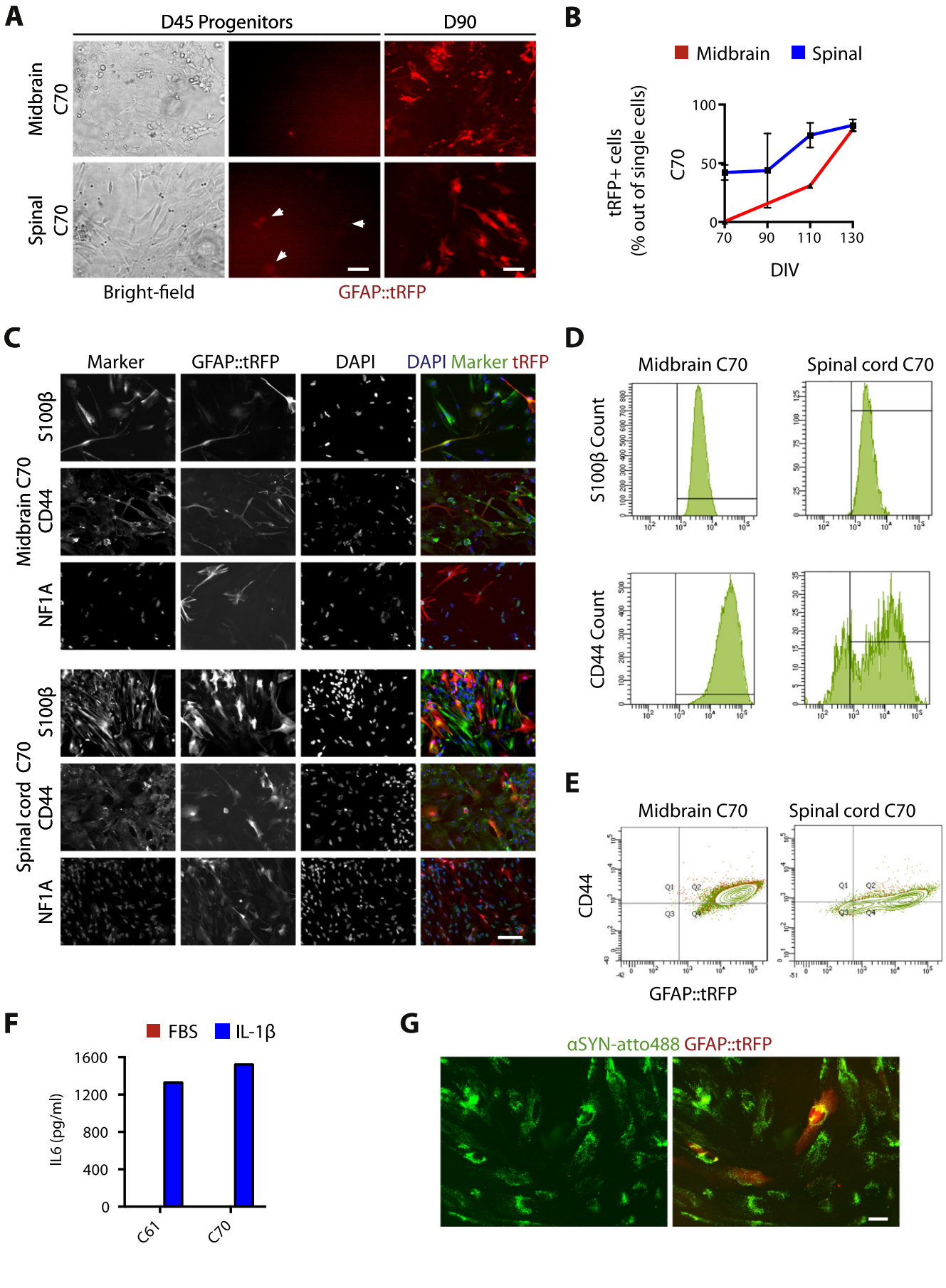
A
D45 Progenitors
D90
Midbrain C70
Spinal C70
Bright-field
GFAP::tRFP
B
Midbrain
Spinal
tRFP+ cells (% out of single cells)
C70
100
50
0
70
90
110
130
DIV
C
Marker
GFAP::tRFP
DAPI
DAPI Marker tRFP
Midbrain C70
S100β
CD44
NF1A
Spinal cord C70
S100β
CD44
NF1A
D
Midbrain C70
Spinal cord C70
S100β Count
CD44 Count
E
Midbrain C70
Spinal cord C70
CD44
GFAP::tRFP
F
FBS
IL-1β
IL6 (pg/ml)
1600
1200
800
400
0
C61
C70
G
αSYN-atto488 GFAP::tRFP

specificity of reporter expression using the GFA_{ABC1D} promoter that lacks several regulatory elements resulted in the loss of large quantities of astrocytes, perhaps also revealing astrocyte heterogeneity within the culture.

Interestingly, at day 45 of differentiation, no *GFA_{ABC1D}::TagRFP* positive cells were observed in cultures of any clones differentiated using the midbrain protocol. In marked contrast, *GFA_{ABC1D}::TagRFP* positive cells were observed in cultures aged 45 DIV for several clones differentiated using the spinal cord protocol. Moreover, TagRFP expression was stronger in spinal cord astrocyte cultures than midbrain astrocytes, for the majority of the clones tested (data not shown). These findings were common to both hESC and hiPSC, and may reflect the dynamic expression of the promoter, in different part of the central nervous system. Similar to our observation was that of Gu and coworkers who showed that in wildtype mice, GFAP expression is much stronger in the spinal cord than in the brainstem (Gu et al., 2010). Nonetheless, even if TagRFP expression appeared to be more prominent and more robust in and between spinal cord clones compared to midbrain clones, purification of TagRFP-expressing astrocytes generated using either of the protocols resulted in homogeneous populations of astrocytes expressing canonical markers NF1A, CX43, GLAST, GS, S100β and CD44, We also observed morphological differences and varying staining intensity in Reelin between spinal and midbrain astrocyte cultures (data not shown).

In several instances (especially observed for midbrain clones), the percentages of GFAP-expressing astrocytes and TagRFP-expressing cells in purified cultures aged 130 DIV were lower than the initial FACS-purified *GFA_{ABC1D}::TagRFP*$^+$ astrocytes (Fig. 4A). This could be attributed to GFAP down-regulation in maturing astrocytes (Roybon et al., 2013). Moreover, the difference between reporter expression and endogenous GFAP can be attributed to half-lives of intermediate filament proteins in astrocytes which are most likely relatively short (Chiu and Goldman, 1984) compared to stable fluorescent proteins such as TagRFP. Nevertheless, the clones we selected (C32 for hESC and C70 for hiPSC) showed high overlap between GFAP and TagRFP, and their purification by FACS resulted in homogeneous cultures of astrocytes expressing canonical astroglial markers.

Notably, astrocytes generated from the human ESC reporter line could be used in several assays. Interestingly, almost all cytokines and chemokines detected in the protein array study were also detected in a recent similar study employing human fetal astrocytes (Choi et al., 2014). In concordance with our data, Choi and coworkers found MCP-1 secretion reduced. In contrast, while our data indicated no change in MIF secretion between FBS and IL-1β treated cultures, they reported that the secretion of this anti-inflammatory cytokine decreased following a one-day treatment period with two cytokines: IL-1β and TNFα. This decrease in MIF secretion may only be detectable after short treatment, or attributed to the presence of TNFα. Nevertheless, all other cytokines and chemokines were commonly secreted in both studies. It is worth mentioning that our new models have additional uses, such as the tracking of pathogenic protein labeled with ATTO488 in astrocytes in unpurified cultures, where astrocytes generated from regionalized progenitors are labeled using *GFAP::TagRFP*.

Together, our findings indicate that the lines we generated to report on astrocytes could be useful for future studies of neuroinflammation and astrocyte diversity. Moreover, they provide a new platform to study the dynamics of pathogenic proteins aggregation or their transfer in and between living human astrocytes.

Finally, as a proof-of-principle, we showed that the reporter lines could also be generated using human iPSCs. The hiPSC reporter lines differentiated with the spinal cord and midbrain protocols generated astrocytes strongly resembled those generated from hESC, as previously reported for other hESC and hiPSC lines (Roybon et al., 2013). The hiPSC clone C70 generated astrocytes responding to IL-1β treatment, assessed by ELISA for IL-6 secretion, and able to take up α-synuclein protein (Fig. 7E).

In this study, we have shown that the human *GFA_{ABC1D}* promoter can be used to generate stable hPSC lines to report on GFAP-expressing astrocytes. Furthermore, we have shown that purification of fluorescently labeled astrocytes enables enrichment of regionally defined GFAP$^+$ astrocytes. These new cellular models therefore offer an unprecedented opportunity to investigate human astrocyte biology in a finer and easier way, and provide a platform for the isolation of hPSC-derived GFAP$^+$ astrocytes for multiple purposes. Furthermore, the fact that these were engineered to express TagRFP provides an advantage for transplantation studies (Davies et al., 2011; Lepore et al., 2008), especially in transgenic animal models where specific neuronal subtypes are labeled with green-fluorescent protein (GFP). Our cellular models will also be of great interest for co-culture studies with GFP-labeled neurons, and to follow uptake and degradation of fluorescently labeled pathogenic proteins using live imaging. We envision

Figure 7 Generation and characterization of GFA_{ABC1D}::TagRFP report line for the reporting on astrocytes generated from iPSC derived progenitors. A. Absence of reporter expression in iPSC-derived C70 midbrain, but not spinal cultures, at 45 DIV (white arrowheads pinpoint at). Reporter expression is detected at 90 DIV in the same cultures. Scale bars represent 20 μm. B. Time course study showing the percent of *GFA_{ABC1D}::TagRFP* positive cells out of live single cells (measured by FACS), for C70 using midbrain (red) and spinal cord (blue) protocol, measured by flow cytometry. Mean ± s.e.m.; n = 3 separate differentiations for spinal cord astrocytes and n = 1 for midbrain astrocytes. C. Canonical markers S100β, CD44 and NF1A expression in astrocytes aged 130 DIV generated using midbrain (upper panels) and spinal cord (lower panels) protocols. Scale bar represent 50 μm. D. Flow cytometry analysis of midbrain and spinal cord cultures stained for S100β and CD44 show enrichment in purified cultures grown for 40 additional days *in vitro*. Graphs show number of FITC positive cells above threshold. E. Flow cytometry analysis confirms enrichment of TagRFP/CD44 co-expressing astrocytes clone 70 midbrain (left) and spinal cord (right) cultures, 40 days post-FACS-purification. F. Purified astrocytes aged 130 DIV treated with IL-1β release IL-6, measured by ELISA (shown for C70 and another clone, C61). G. Cellular localization of aSYN in 90 DIV live unpurified iPSC-derived spinal cord astrocyte cultures (C70) treated for 4 days with ATTO488-labeled aSYN monomers. Scale bar represents 10 μm.

that the generation of reporter lines for the isolation of specific cell types will become a powerful tool for the development of bio-diagnostic tools, with focus on personal disparities in health and disease. Moreover, our strategy could be adjusted to include Cre-lox flanking sites, enabling excision of reporter cassette, for transplantation of pure non-labeled human astocytes in the brain.

Acknowledgments

We thank M. Brenner and H. Wichterle who generously provided the GFA_{ABC1D} promoter and the TagRFP-PGK::Neo vector, respectively.

We thank R. Sattler and F. Casagrande for the critical reading of the manuscript.

This work was supported by the Strong Research Environment MultiPark (multidisciplinary research on Parkinson's disease at Lund University), and grants to L.R. from the following foundations: The Swedish Parkinson Foundation (Parkinsonfonden), Holger Crafoord Foundation, Åke Wibergs Foundation, Magnus Bergvalls Foundation, Greta och Johan Kocks Foundation, and donations for science, medicine and technology at Fysiografen in Lund. L.R. is a young investigator supported by the Strong Research Environment MultiPark at Lund University, and partner of the Brainstem, Stem Cell Center for Excellence in Neurology funded by the Innovation fund Denmark.

S.H. and M.B. performed experiments and analysis. M.D. assisted with qPCR and M.D. and A.H. assisted with FACS. A.G.D. generated the *GFA_{ABC1D}::TagRFP-PGK::Neo* construct. M.J.D., T.K. and K.F. provided reagents and input on experiments. S.H, M.B. and L.R. conceived the experiments and wrote the manuscript. All authors gave input on the manuscript and approved its final version.

Appendix A. Supplementary data

Supplementary data to this article can be found online at http://dx.doi.org/10.1016/j.scr.2015.05.014.

References

Anderson, M.A., Ao, Y., Sofroniew, M.V., 2014. Heterogeneity of reactive astrocytes. Neurosci. Lett. 565, 23–29.

Attwell, D., Buchan, A.M., Charpak, S., Lauritzen, M., Macvicar, B.A., Newman, E.A., 2010. Glial and neuronal control of brain blood flow. Nature 468, 232–243.

Bachoo, R.M., Kim, R.S., Ligon, K.L., Maher, E.A., Brennan, C., Billings, N., Chan, S., Li, C., Rowitch, D.H., Wong, W.H., et al., 2004. Molecular diversity of astrocytes with implications for neurological disorders. Proc. Natl. Acad. Sci. U. S. A. 101, 8384–8389.

Bousset, L., Pieri, L., Ruiz-Arlandis, G., Gath, J., Jensen, P.H., Habenstein, B., Madiona, K., Olieric, V., Bockmann, A., Meier, B.H., et al., 2013. Structural and functional characterization of two alpha-synuclein strains. Nat. Commun. 4, 2575.

Brenner, M., 1994. Structure and transcriptional regulation of the GFAP gene. Brain Pathol. 4, 245–257.

Chaboub, L.S., Deneen, B., 2012. Developmental origins of astrocyte heterogeneity: the final frontier of CNS development. Dev. Neurosci. 34, 379–388.

Chambers, S.M., Fasano, C.A., Papapetrou, E.P., Tomishima, M., Sadelain, M., Studer, L., 2009. Highly efficient neural conversion of human ES and iPS cells by dual inhibition of SMAD signaling. Nat. Biotechnol. 27, 275–280.

Chao, C.C., Hu, S., Sheng, W.S., Bu, D., Bukrinsky, M.I., Peterson, P.K., 1996. Cytokine-stimulated astrocytes damage human neurons via a nitric oxide mechanism. Glia 16, 276–284.

Chen, Y., Swanson, R.A., 2003. Astrocytes and brain injury. J. Cereb. Blood Flow Metab. 23, 137–149.

Chiu, F.C., Goldman, J.E., 1984. Synthesis and turnover of cytoskeletal proteins in cultured astrocytes. J. Neurochem. 42, 166–174.

Chizhikov, V.V., Millen, K.J., 2004. Control of roof plate formation by Lmx1a in the developing spinal cord. Development 131, 2693–2705.

Choi, H.B., Gordon, G.R., Zhou, N., Tai, C., Rungta, R.L., Martinez, J., Milner, T.A., Ryu, J.K., McLarnon, J.G., Tresguerres, M., et al., 2012. Metabolic communication between astrocytes and neurons via bicarbonate-responsive soluble adenylyl cyclase. Neuron 75, 1094–1104.

Choi, S.S., Lee, H.J., Lim, I., Satoh, J., Kim, S.U., 2014. Human astrocytes: secretome profiles of cytokines and chemokines. PLoS One 9, e92325.

Davies, S.J., Shih, C.H., Noble, M., Mayer-Proschel, M., Davies, J.E., Proschel, C., 2011. Transplantation of specific human astrocytes promotes functional recovery after spinal cord injury. PLoS One 6, e17328.

Deneen, B., Ho, R., Lukaszewicz, A., Hochstim, C.J., Gronostajski, R.M., Anderson, D.J., 2006. The transcription factor NFIA controls the onset of gliogenesis in the developing spinal cord. Neuron 52, 953–968.

Devine, M.J., Ryten, M., Vodicka, P., Thomson, A.J., Burdon, T., Houlden, H., Cavaleri, F., Nagano, M., Drummond, N.J., Taanman, J.W., et al., 2011. Parkinson's disease induced pluripotent stem cells with triplication of the alpha-synuclein locus. Nat. Commun. 2, 440.

Di Giorgio, F.P., Boulting, G.L., Bobrowicz, S., Eggan, K.C., 2008. Human embryonic stem cell-derived motor neurons are sensitive to the toxic effect of glial cells carrying an ALS-causing mutation. Cell Stem Cell 3, 637–648.

Episcopo, F.L., Tirolo, C., Testa, N., Caniglia, S., Morale, M.C., Marchetti, B., 2013. Reactive astrocytes are key players in nigrostriatal dopaminergic neurorepair in the MPTP mouse model of Parkinson's disease: focus on endogenous neurorestoration. Curr. Aging Sci. 6, 45–55.

Eroglu, C., Barres, B.A., 2010. Regulation of synaptic connectivity by glia. Nature 468, 223–231.

Fischer, Y., Ganic, E., Ameri, J., Xian, X., Johannesson, M., Semb, H., 2010. NANOG reporter cell lines generated by gene targeting in human embryonic stem cells. PLoS One 5.

Gu, X.L., Long, C.X., Sun, L., Xie, C., Lin, X., Cai, H., 2010. Astrocytic expression of Parkinson's disease-related A53T alpha-synuclein causes neurodegeneration in mice. Mol. Brain 3, 12.

Haidet-Phillips, A.M., Hester, M.E., Miranda, C.J., Meyer, K., Braun, L., Frakes, A., Song, S., Likhite, S., Murtha, M.J., Foust, K.D., et al., 2011. Astrocytes from familial and sporadic ALS patients are toxic to motor neurons. Nat. Biotechnol. 29, 824–828.

Han, X., Chen, M., Wang, F., Windrem, M., Wang, S., Shanz, S., Xu, Q., Oberheim, N.A., Bekar, L., Betstadt, S., et al., 2013. Forebrain engraftment by human glial progenitor cells enhances synaptic plasticity and learning in adult mice. Cell Stem Cell 12, 342–353.

Hochstim, C., Deneen, B., Lukaszewicz, A., Zhou, Q., Anderson, D.J., 2008. Identification of positionally distinct astrocyte subtypes whose identities are specified by a homeodomain code. Cell 133, 510–522.

Hu, B.Y., Weick, J.P., Yu, J., Ma, L.X., Zhang, X.Q., Thomson, J.A., Zhang, S.C., 2010. Neural differentiation of human induced pluripotent stem cells follows developmental principles but with variable potency. Proc. Natl. Acad. Sci. U. S. A. 107, 4335–4340.

Jiang, P., Chen, C., Wang, R., Chechneva, O.V., Chung, S.H., Rao, M.S., Pleasure, D.E., Liu, Y., Zhang, Q., Deng, W., 2013. hESC-derived Olig2+ progenitors generate a subtype of astroglia with protective effects against ischaemic brain injury. Nat. Commun. 4, 2196.

Juopperi, T.A., Kim, W.R., Chiang, C.H., Yu, H., Margolis, R.L., Ross, C.A., Ming, G.L., Song, H., 2012. Astrocytes generated from patient induced pluripotent stem cells recapitulate features of Huntington's disease patient cells. Mol. Brain 5, 17.

Kiecker, C., Lumsden, A., 2012. The role of organizers in patterning the nervous system. Annu. Rev. Neurosci. 35, 347–367.

Kirkeby, A., Grealish, S., Wolf, D.A., Nelander, J., Wood, J., Lundblad, M., Lindvall, O., Parmar, M., 2012a. Generation of regionally specified neural progenitors and functional neurons from human embryonic stem cells under defined conditions. Cell Rep. 1, 703–714.

Kirkeby, A., Nelander, J., Parmar, M., 2012b. Generating regionalized neuronal cells from pluripotency, a step-by-step protocol. Front. Cell. Neurosci. 6, 64.

Kondo, T., Asai, M., Tsukita, K., Kutoku, Y., Ohsawa, Y., Sunada, Y., Imamura, K., Egawa, N., Yahata, N., Okita, K., et al., 2013. Modeling Alzheimer's disease with iPSCs reveals stress phenotypes associated with intracellular Abeta and differential drug responsiveness. Cell Stem Cell 12, 487–496.

Krencik, R., Weick, J.P., Liu, Y., Zhang, Z.J., Zhang, S.C., 2011. Specification of transplantable astroglial subtypes from human pluripotent stem cells. Nat. Biotechnol. 29, 528–534.

Kriks, S., Shim, J.W., Piao, J., Ganat, Y.M., Wakeman, D.R., Xie, Z., Carrillo-Reid, L., Auyeung, G., Antonacci, C., Buch, A., et al., 2011. Dopamine neurons derived from human ES cells efficiently engraft in animal models of Parkinson's disease. Nature 480, 547–551.

Lamas, N.J., Johnson-Kerner, B., Roybon, L., Kim, Y.A., Garcia-Diaz, A., Wichterle, H., Henderson, C.E., 2014. Neurotrophic requirements of human motor neurons defined using amplified and purified stem cell-derived cultures. PLoS One 9, e110324.

Lee, Y., Messing, A., Su, M., Brenner, M., 2008. GFAP promoter elements required for region-specific and astrocyte-specific expression. Glia 56, 481–493.

Lee, H.J., Suk, J.E., Patrick, C., Bae, E.J., Cho, J.H., Rho, S., Hwang, D., Masliah, E., Lee, S.J., 2010. Direct transfer of alpha-synuclein from neuron to astroglia causes inflammatory responses in synucleinopathies. J. Biol. Chem. 285, 9262–9272.

Lee, M., McGeer, E., McGeer, P.L., 2013. Neurotoxins released from interferon-gamma-stimulated human astrocytes. Neuroscience 229, 164–175.

Lek, M., Dias, J.M., Marklund, U., Uhde, C.W., Kurdija, S., Lei, Q., Sussel, L., Rubenstein, J.L., Matise, M.P., Arnold, H.H., et al., 2010. A homeodomain feedback circuit underlies step-function interpretation of a Shh morphogen gradient during ventral neural patterning. Development 137, 4051–4060.

Lepore, A.C., Rauck, B., Dejea, C., Pardo, A.C., Rao, M.S., Rothstein, J.D., Maragakis, N.J., 2008. Focal transplantation-based astrocyte replacement is neuroprotective in a model of motor neuron disease. Nat. Neurosci. 11, 1294–1301.

Liu, Y., Jiang, P., Deng, W., 2011. OLIG gene targeting in human pluripotent stem cells for motor neuron and oligodendrocyte differentiation. Nat. Protoc. 6, 640–655.

Nelson, A.D., Suzuki, M., Svendsen, C.N., 2008. A high concentration of epidermal growth factor increases the growth and survival of neurogenic radial glial cells within human neurosphere cultures. Stem Cells 26, 348–355.

Oberheim, N.A., Takano, T., Han, X., He, W., Lin, J.H., Wang, F., Xu, Q., Wyatt, J.D., Pilcher, W., Ojemann, J.G., et al., 2009. Uniquely hominid features of adult human astrocytes. J. Neurosci. 29, 3276–3287.

Pekny, M., Wilhelmsson, U., Pekna, M., 2014. The dual role of astrocyte activation and reactive gliosis. Neurosci. Lett. 565, 30–38.

Placantonakis, D.G., Tomishima, M.J., Lafaille, F., Desbordes, S.C., Jia, F., Socci, N.D., Viale, A., Lee, H., Harrison, N., Tabar, V., et al., 2009. BAC transgenesis in human embryonic stem cells as a novel tool to define the human neural lineage. Stem Cells 27, 521–532.

Reyes, J.F., Rey, N.L., Bousset, L., Melki, R., Brundin, P., Angot, E., 2014. Alpha-synuclein transfers from neurons to oligodendrocytes. Glia 62, 387–398.

Ribes, V., Balaskas, N., Sasai, N., Cruz, C., Dessaud, E., Cayuso, J., Tozer, S., Yang, L.L., Novitch, B., Marti, E., et al., 2010. Distinct Sonic Hedgehog signaling dynamics specify floor plate and ventral neuronal progenitors in the vertebrate neural tube. Genes Dev. 24, 1186–1200.

Rostovskaya, M., Fu, J., Obst, M., Baer, I., Weidlich, S., Wang, H., Smith, A.J., Anastassiadis, K., Stewart, A.F., 2012. Transposon-mediated BAC transgenesis in human ES cells. Nucleic Acids Res. 40, e150.

Rowitch, D.H., Kriegstein, A.R., 2010. Developmental genetics of vertebrate glial-cell specification. Nature 468, 214–222.

Roybon, L., Lamas, N.J., Garcia-Diaz, A., Yang, E.J., Sattler, R., Jackson-Lewis, V., Kim, Y.A., Kachel, C.A., Rothstein, J.D., Przedborski, S., et al., 2013. Human stem cell-derived spinal cord astrocytes with defined mature or reactive phenotypes. Cell Rep. 4, 1035–1048.

Schuldiner, M., Yanuka, O., Itskovitz-Eldor, J., Melton, D.A., Benvenisty, N., 2000. Effects of eight growth factors on the differentiation of cells derived from human embryonic stem cells. Proc. Natl. Acad. Sci. U. S. A. 97, 11307–11312.

Semple, B.D., Frugier, T., Morganti-Kossmann, M.C., 2010. CCL2 modulates cytokine production in cultured mouse astrocytes. J. Neuroinflammation 7, 67.

Serio, A., Bilican, B., Barmada, S.J., Ando, D.M., Zhao, C., Siller, R., Burr, K., Haghi, G., Story, D., Nishimura, A.L., et al., 2013. Astrocyte pathology and the absence of non-cell autonomy in an induced pluripotent stem cell model of TDP-43 proteinopathy. Proc. Natl. Acad. Sci. U. S. A. 110, 4697–4702.

Shaltouki, A., Peng, J., Liu, Q., Rao, M.S., Zeng, X., 2013. Efficient generation of astrocytes from human pluripotent stem cells in defined conditions. Stem Cells 31, 941–952.

Simard, M., Nedergaard, M., 2004. The neurobiology of glia in the context of water and ion homeostasis. Neuroscience 129, 877–896.

Swistowski, A., Peng, J., Liu, Q., Mali, P., Rao, M.S., Cheng, L., Zeng, X., 2010. Efficient generation of functional dopaminergic neurons from human induced pluripotent stem cells under defined conditions. Stem Cells 28, 1893–1904.

Tsai, H.H., Li, H., Fuentealba, L.C., Molofsky, A.V., Taveira-Marques, R., Zhuang, H., Tenney, A., Murnen, A.T., Fancy, S.P., Merkle, F., et al., 2012. Regional astrocyte allocation regulates CNS synaptogenesis and repair. Science 337, 358–362.

Waak, J., Weber, S.S., Waldenmaier, A., Gorner, K., Alunni-Fabbroni, M., Schell, H., Vogt-Weisenhorn, D., Pham, T.T., Reumers, V., Baekelandt, V., et al., 2009. Regulation of astrocyte inflammatory responses by the Parkinson's disease-associated gene DJ-1. FASEB J. 23, 2478–2489.

Wakabayashi, K., Hayashi, S., Yoshimoto, M., Kudo, H., Takahashi, H., 2000. NACP/alpha-synuclein-positive filamentous inclusions in astrocytes and oligodendrocytes of Parkinson's disease brains. Acta Neuropathol. 99, 14–20.

Wichterle, H., Przedborski, S., 2010. What can pluripotent stem cells teach us about neurodegenerative diseases? Nat. Neurosci. 13, 800–804.

Yamanaka, K., Chun, S.J., Boillee, S., Fujimori-Tonou, N., Yamashita, H., Gutmann, D.H., Takahashi, R., Misawa, H., Cleveland, D.W., 2008. Astrocytes as determinants of disease progression in inherited amyotrophic lateral sclerosis. Nat. Neurosci. 11, 251–253.

Yan, Y., Ding, X., Li, K., Ciric, B., Wu, S., Xu, H., Gran, B., Rostami, A., Zhang, G.X., 2012. CNS-specific therapy for ongoing EAE by silencing IL-17 pathway in astrocytes. Mol. Ther. 20, 1338–1348.

Yuan, S.H., Martin, J., Elia, J., Flippin, J., Paramban, R.I., Hefferan, M.P., Vidal, J.G., Mu, Y., Killian, R.L., Israel, M.A., et al., 2011. Cell-surface marker signatures for the isolation of neural stem cells, glia and neurons derived from human pluripotent stem cells. PLoS One 6, e17540.

Zhang, W., Wang, T., Pei, Z., Miller, D.S., Wu, X., Block, M.L., Wilson, B., Zhang, W., Zhou, Y., Hong, J.S., et al., 2005. Aggregated alpha-synuclein activates microglia: a process leading to disease progression in Parkinson's disease. FASEB J. 19, 533–542.